frontiers | Frontiers in Chemistry

TYPE Mini Review
PUBLISHED 07 April 2023
DOI 10.3389/fchem.2023.1174207

Gas sensing performance of In_2O_3 nanostructures: A mini review

Shulin Yang[1,2], Huan Yin[1], Zhao Wang[2], Gui Lei[1], Huoxi Xu[1], Zhigao Lan[1]* and Haoshuang Gu[2]*

[1]Hubei Key Laboratory for Processing and Application of Catalytic Materials, School of Physics and Electronic Information, Huanggang Normal University, Huanggang, China, [2]Hubei Key Laboratory of Ferro and Piezoelectric Materials and Devices, Faculty of Physics and Electronic Sciences, Hubei University, Wuhan, China

OPEN ACCESS

EDITED BY
Yanqiong Li,
Chongqing University of Arts and Sciences, China

REVIEWED BY
Pengfei Jia,
Guangxi University, China

*CORRESPONDENCE
Zhigao Lan,
✉ lanzhg@hgnu.edu.cn
Haoshuang Gu,
✉ guhsh@hubu.edu.cn

SPECIALTY SECTION
This article was submitted to Nanoscience, a section of the journal Frontiers in Chemistry

RECEIVED 26 February 2023
ACCEPTED 31 March 2023
PUBLISHED 07 April 2023

CITATION
Yang S, Yin H, Wang Z, Lei G, Xu H, Lan Z and Gu H (2023), Gas sensing performance of In_2O_3 nanostructures: A mini review.
Front. Chem. 11:1174207.
doi: 10.3389/fchem.2023.1174207

Effective detection of toxic and hazardous gases is crucial for ensuring human safety, and high-performance metal oxide-based gas sensors play an important role in achieving this goal. In_2O_3 is a widely used n-type metal oxide in gas sensors, and various In_2O_3 nanostructures have been synthesized for detecting small gas molecules. In this review, we provide a brief summary of current research on In_2O_3-based gas sensors. We discuss methods for synthesizing In_2O_3 nanostructures with various morphologies, and mainly review the sensing behaviors of these structures in order to better understand their potential in gas sensors. Additionally, the sensing mechanism of In_2O_3 nanostructures is discussed. Our review further indicates that In_2O_3-based nanomaterials hold great promise for assembling high-performance gas sensors.

KEYWORDS

In_2O_3, nanostructrues, gas sensor, sensing mechanism, review

1 Introduction

In recent decades, there has been growing attention to the effective monitoring of air quality due to the increasingly serious environmental problems (Ma et al., 2016; Zhang et al., 2018; Ge et al., 2019). Even toxic gases with low concentrations can be harmful to human health (Park et al., 2016; Cordero et al., 2018; Zhou et al., 2022). For example, the toxic gas formaldehyde (HCHO) can cause serious blurred vision and vertigo when its concentration exceeds 0.1 mg/m^3 (Peng and Huang, 2022). In the workplace, the concentration of n-butanol should be kept below 152 mg/m^3 to ensure the safety of human lives (Zhao et al., 2021). In addition, a high risk of explosion may occur if the concentration of H_2 reaches 4%–75% in the air (Phanichphant, 2014). It should be noted that many toxic, hazardous, or flammable gases are odorless, colorless, and tasteless, which means they cannot be detected by humans directly (Wetchakun et al., 2011; Chi et al., 2014; Shi et al., 2018). Therefore, high-performance gas sensors are of great importance to effectively detect these gases and their concentrations in the air.

Metal oxide-based gas sensors have become a popular research topic in recent years due to their advantages of low cost, easy of fabrication, low power consumption and high sensor response to a wide range of gases (Xu and Cheng, 2016; Lu et al., 2019; Nikolic et al., 2020). Nanostructured metal oxides always presented high specific surface areas and could provide abundant active sites on their surfaces (Zhang et al., 2017; Srinivasan et al., 2019; Walker et al., 2019). This positive factor effectively promotes the adsorption and the diffusion of gas molecules in the sensing materials, resulting in the excellent gas sensing performances of nanostructured metal oxides. For instance, in the study conducted by Zhu et al., CuO nanoflowers demonstrated a significantly higher sensor response of 123.4 to 50 ppm H_2S at

80°C compared to CuO-based microspheres, which only showed a sensor response of 4.36 (Hu et al., 2017; Hu et al., 2018a). Chen et al. also reported superior sensing performance of ZnO-based nanostructures with a sensor response as high as 6043 to 100 ppm triethylamine (TEA) at an optimal working temperature of 183.5°C, when compared to ZnO films (with a response of ~22.5) or hierarchical ZnO microspheres (with a response of 242) (Shen et al., 2018; Liu et al., 2021a; Li et al., 2021). Furthermore, the net-like SnO_2 nanoarrays showed a response time of only 16.3 s to 10 ppm H_2S at 350°C, which was approximately ten times lower than that of SnO_2 films (167.8 s) (Ge et al., 2022). Thus, outstanding gas sensing properties could be expected through synthesizing nanostructured metal oxides.

In_2O_3 is another popular n-type metal oxide that possesses a wide band gap of 3.5–3.7 eV (Vuong et al., 2014; Han et al., 2015; Park, 2017). Its outstanding thermal stability, high conductivity, and excellent chemical/physical properties make it a promising candidate for gas detection (Liang et al., 2015; Kumar et al., 2021; Meng et al., 2022). For example, Zhang et al. successfully prepared Ni-doped In_2O_3-based nanocubes through a hydrothermal method, achieving effective detection of 20 ppm HCHO with a response time of 76 s at room temperature (Zhang et al., 2020). The research conducted by Han et al. demonstrated that the sensor response of In_2O_3 nanorods doped with Co could be improved to 23.2 towards 10 ppm HCHO at 130 C (Wang et al., 2018). Additionally, flower-like In_2O_3 nanomaterials exhibited a sensor response and response time of 3.1 and 53 s, respectively, to 0.5 ppm isoprene at 190°C (Han et al., 2020). A Google Scholar survey with keywords of "nano + In_2O_3+gas sensor" revealed that from 2017 to 2022, there were 826, 878, 919, 1060, 1210, and 1520 papers published on the topic. Although the data obtained may not be entirely accurate, the increasing number of published references highlights the growing attention given to In_2O_3-based gas sensors in recent years. Therefore, summarizing the recent developments in In_2O_3-based gas sensors would be meaningful to better understand their advantages in gas sensing.

In this paper, we have chosen several highly cited published references to conduct a mini review on typical In_2O_3-based gas sensors. Our focus was mainly on summarizing and comparing the high-performance characteristics of these gas sensors. Furthermore, we presented the methods used to prepare various In_2O_3-based materials. Additionally, we provided a brief review of the gas sensing mechanism for In_2O_3-based gas sensors.

2 Research status of gas sensing performances of recent In_2O_3 nanostructures

2.1 Pristine In_2O_3-based nanomaterials

A novel self-heated gas sensor for detecting ethanol at room temperature was assembled by Nguyen et al. using In_2O_3 nanowires (Son et al., 2022). The sensor utilized the Joule effect generated by the In_2O_3 nanowires under an operating voltage to achieve self-heating during operation. The In_2O_3 nanowires were synthesized *via* a one-chip growth technique of thermal evaporation. The gap between the prepared electrodes was designed to be 10, 30 or 40 μm (Figures 1A, B), with the corresponding devices labeled as sensor-10, sensor-30, or sensor-40, respectively. Results showed that the well-crystallized In_2O_3 nanowires were successful to bridge the gap of electrodes (Figures 1C–E). The In_2O_3 nanowires had an average diameter of ~100 nm and an average length of over 10 μm (Figure 1F). Sensor-40 exhibited better ethanol sensing performance compared to sensor-10 or sensor-30. Sensor-40 showed a superior sensing performance to 10–2000 ppm ethanol compared to NH_3 under a supplied power of 1.06 mW (Figures 1G–J). The sensor response of sensor-40–2000 ppm ethanol was ~1.45. Meanwhile, the sensor response of sensor-40–1000 ppm ethanol was higher than that to 1000 ppm acetone, CO, H_2S or NH_3 (Figure 1K), indicating good gas selectivity of the In_2O_3 nanowires. Additionally, the sensor response of sensor-40 to ethanol was not significantly affected by humidity levels of 60%, 70%, or 80% (Figure 1L).

Shboul et al. have developed a novel gas sensor mainly composed of solution-printed In2O3 nanoparticles (Al Shboul and Izquierdo, 2021). In their study, In_2O_3 nanoparticles, copper acetate (CuAc), graphite (Gt) flakes, and polystyrene (PS) were added to 10 mL of xylene to form a stable paste. The paste was then spread over a flexible PET substrate with prepared carbon electrodes to assemble the gas sensor. The In_2O_3-based sensor (SS), without CuAc, showed unresponsive sensing performance to H_2S showed unresponsive sensing behavior towards H_2S with concentrations below 100 ppb. The sensor response of the SS was only 2–100 ppb H_2S, and the response time was as long as ~25 min. The In_2O_3-based sensing material with 10 wt% CuAc (MS10) exhibited better sensing performance than sensing materials with 2 wt% CuAc (MS2), 25 wt % CuAc (MS25), or 50 wt% CuAc (MS50). The sensor response of the MS10 was found to be ~18–100 ppm H_2S at room temperature, with a relative humidity of ~30%.

The study by Pham et al. also showed the potential of porous In_2O_3 nanorods for detecting CO gas at 350°C (Van Tong et al., 2021). The nanorods were synthesized *via* a hydrothermal method at 180°C for 10 h, and showed a sensor response of 3.46–400 ppm CO with a response and recovery time of 41/43 s. Similarly, Zhang et al. employed a surfactant-assisted co-precipitation method to prepare hierarchical branch-like In_2O_3 nanomaterial for detecting ozone (O_3) (Sui et al., 2021). The resulting hierarchical branch-like In_2O_3 showed a high sensor response of 44–100 ppb O_3 at its optimum working temperature of 70°C.

2.2 In_2O_3-based composites

2.2.1 In_2O_3 composited with noble metals

Wang et al. have investigated the impacts of Au, Ag, Pt, and Pd on the ethanol gas sensing performance of long-range mesoporous In_2O_3 (Cheng et al., 2021). They synthesized the ordered mesoporous In_2O_3 by replicating the structure of SBA-15, and then prepared Au, Ag, Pt, or Pd-doped In_2O_3 through an *in-situ* doping routine. The mesoporous In_2O_3 doped with Pd exhibited a specific surface area of 94.22 m^2/g, significantly higher than that of pristine In_2O_3 (64.55 m^2/g), Au-doped In_2O_3 (78.29 m^2/g), Ag-doped In_2O_3 (67.52 m^2/g), or Pt-doped In_2O_3 (76.41 m^2/g). Similarly, the pore diameter for the Pd-doped In_2O_3 was 3.6 nm, also larger than that for pristine In_2O_3 (2.6 nm). The high specific

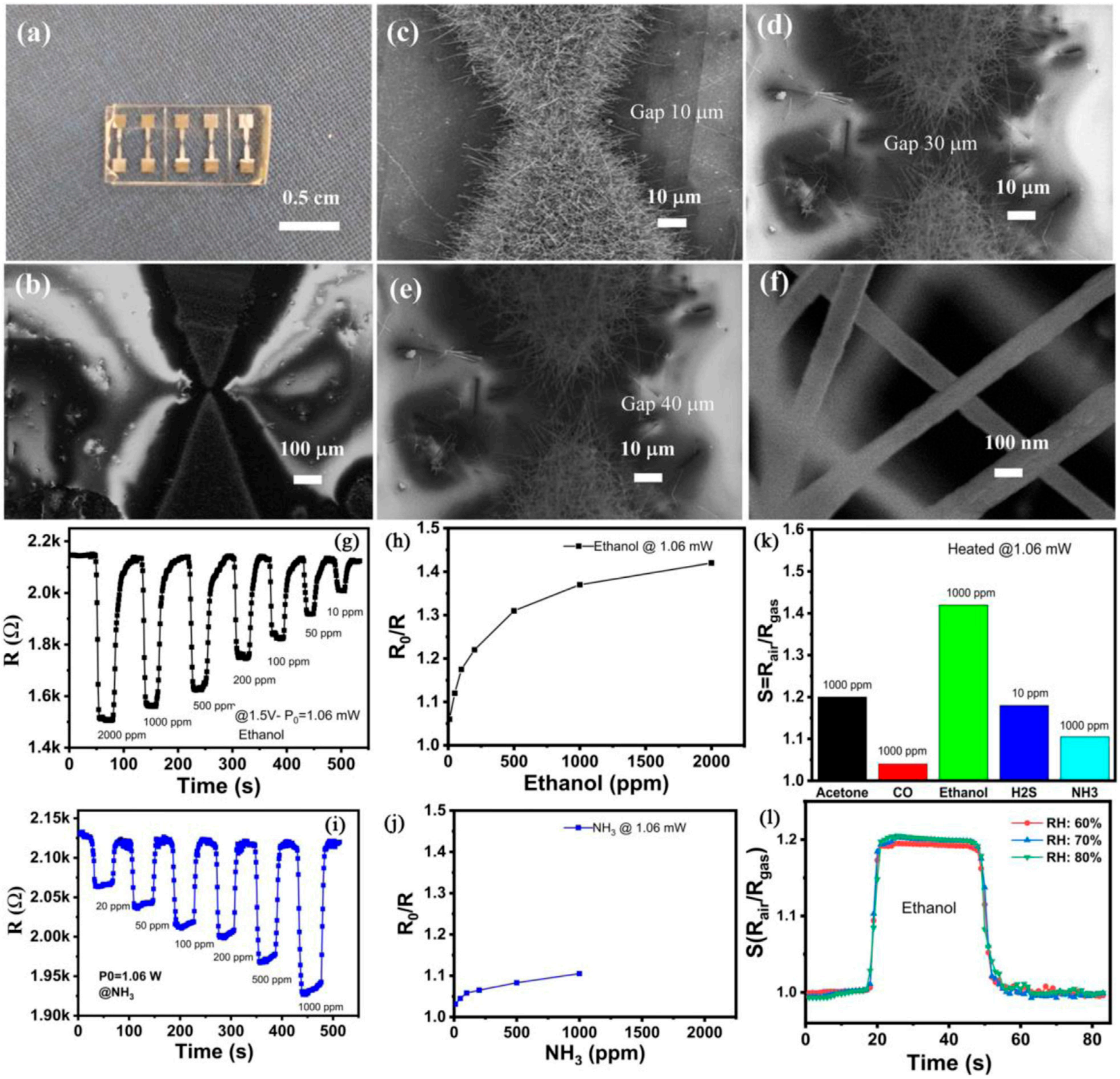

FIGURE 1
(A) Digital image of the assembled gas sensor. **(B)** SEM image of a gas sensor. **(C–E)** SEM image of In_2O_3 nanowires grown at electrodes with gasps of 10, 30 and 40 µm, respectively. **(F)** High magnification SEM of In_2O_3 nanowires. **(G, H)** Dynamic gas sensing performance and sensor response **(I, J)** of sensor-40 to 10–2000 ppm ethanol or NH_3 at room temperature. **(K)** Selective gas sensing performance of sensor-40. **(L)** ethanol gas sensing behavior of sensor-40 under different humidity. Reprinted with permission from ref. (Son et al., 2022). Copyright 2022, Elsevier.

surface area and large pore diameter are favorable for improving gas molecule adsorption and diffusion in the sensing material. Consequently, the concentration of chemisorbed oxygen species in Pd-doped In_2O_3 was the highest among all samples, reaching 54.8%. The sensor based on Pd-doped In_2O_3 also demonstrated the best performance for 100 ppm ethanol at an operating temperature of 200–350°C. The sensor response of Pd-doped In_2O_3 was 39 at 250°C, higher than that of pristine In_2O_3 (~5), Au-doped In_2O_3 (~7.5), Ag-doped In_2O_3 (~15), or Pt-doped In_2O_3 (~17.5). Furthermore, Pd-doped In_2O_3 exhibited higher sensor response to 100 ppm ethanol than to 100 ppm ammonia, methanol, toluene, benzene, acetone, formaldehyde, or ethanol, revealing excellent sensing selectivity.

The research conducted by Zhang et al. showed that an excellent hydrogen sensing performance could be achieved with the use of Tb-doped In_2O_3 nanocomposites decorated with Ag (Ag-Tb-In_2O_3) (Bai et al., 2022). In their study, the Ag-modified Tb-doped In_2O_3 nanocomposite was successfully synthesized through a hydrothermal process combined with a facile annealing method. Interestingly, the material exhibited two coexisting crystalline phases, including the hexagonal phase In_2O_3 (h-In_2O_3) and the cubic phase In_2O_3 (c-In_2O_3). Further analysis of the XRD patterns confirmed that the Tb was doped within the In_2O_3 while the Ag was decorated on the surface of the nanocomposite. The Tb doping was found to reduce the grain sizes of both c-In_2O_3 and h-In_2O_3, resulting in the generation of oxygen vacancies in the nanocomposite. Consequently, the Ag-Tb-In_2O_3 nanocomposite exhibited a better sensing performance for 500 ppb H_2 at operating temperatures ranging from 120 to 200°C. The sensor response of the Ag-Tb-In_2O_3 was found to be 4.63–500 ppb H_2 at its optimum operating temperature of 160°C, which is higher than that of the pristine In_2O_3 (~1.5), Tb-doped In_2O_3 (~2.5), or Ag-decorated In_2O_3 (~3.5).

2.2.2 In_2O_3 composited with metal oxides

The study by Xie et al. demonstrated that the hydrogen sensing performance of In_2O_3 nanotubes could be significantly enhanced by co-doping them with PdO and NiO (Luo et al., 2021). Pristine In_2O_3 and In_2O_3 doped with NiO, PdO or NiO/PdO were synthesized using an electrospinning method. All four samples exhibited sensing performances to 5 ppm hydrogen gas at 160–300°C. Among them, the PdO/NiO-In_2O_3 nanotubes showed the highest sensor response, with a value of 487.52 to 5 ppm H_2 at 160°C. In contrast, the sensor responses of pristine In_2O_3, NiO-In_2O_3, and PdO-In_2O_3 were lower than 20. The response times of the pristine In_2O_3 and NiO-In_2O_3 were also relatively long, at 153 s and 97 s, respectively, which might not be suitable for rapid detection of hydrogen gas in practical applications. However, the addition of PdO significantly reduced the response time to only 1 s for both PdO-In_2O_3 and PdO/NiO-In_2O_3, demonstrating the effectiveness of PdO in improving the response time of the In_2O_3-based material. Additionally, the incorporation of NiO reduced the recovery time of pristine In_2O_3 (or PdO-In_2O_3) from the original 232 s (or 674 s) to 168 s (or 336 s).

In a study by Wang et al., it was found that the ethanol gas sensing performance of In_2O_3 nanoflowers could be significantly improved by combining them with metal-organic frameworks (MOF)-derived CO_3O_4 (Han et al., 2021). The In_2O_3 nanoflowers were synthesized *via* a hydrothermal route at 150°C for 10 h. At the optimum operating temperature of 280°C, the CO_3O_4-In_2O_3 nanoflowers exhibited a sensor response of over 5000 to 100 ppm ethanol. Similarly, the MOFs-derived porous Au@Cr_2O_3-In_2O_3 nanorods were found to effectively detect 1 ppm isoprene with a sensor response of 6.4 at 180°C (Wu et al., 2022).

2.2.3 In_2O_3 composite with other materials

Song et al. reported an outstanding methanol sensing performance of In_2O_3 nanocubes composited with $Ti_3C_2T_x$ MXene at room temperature (Liu et al., 2021b). The In_2O_3 nanocubes were synthesized *via* a hydrothermal route at 140°C for 24 h, and the multilayer $Ti_3C_2T_x$ MXene was synthesized through etching the bulk MAX (Ti_3AlC_2) phase with 10 mL HF solution (40 wt%). The In_2O_3 nanocubes were modified with a cationic surfactant, (3-aminopropyl) triethoxysilane (APTES), to positively charge their surfaces. The positively charged In_2O_3 nanocubes were then mixed with the $Ti_3C_2T_x$ MXene with negatively charged surfaces, and the mixture was treated under 120°C for a hydrothermal reaction. The $In_2O_3/Ti_3C_2T_x$ composite exhibited typical n-type gas sensing performance to ethanol at room temperature. However, the resistance of the composite after exposure to ethanol was unable to fully recover to its initial level in air, likely because residual methanol was not desorbed from the active site on the surface of the composite at room temperature. The sensor response of the composite to 5 ppm ethanol was ~29.6 with a response/recovery time of 6.5/3.5 s. The composite also showed a promising gas sensing performance to 5–100 ppm ethanol and was not affected by relative humidity of ~25–70%. The functional groups of the $Ti_3C_2T_x$ would be helpful in accelerating the adsorption of ethanol molecules, while the heterojunction between the In_2O_3 and the $Ti_3C_2T_x$ could be another factor improving the ethanol gas sensing performance of the composite.

Song et al. also found that composting In_2O_3 nanospheres with $Ti_3C_2T_x$ MXene nanosheets and Au could improve their HCHO sensing performance (Liu et al., 2022). The Au-$In_2O_3/Ti_3C_2T_x$ composite exhibited a sensor response of approximately 31%, which is higher than that of the pristine $Ti_3C_2T_x$ (only ~3.6%). Additionally, the response time and recovery time of the composite were as short as 5 s and 4 s, respectively, to 5 ppm HCHO at room temperature.

Zhu et al. reported an effective enhancement of the H_2S sensing performance of In_2O_3 nanocubes through the use of carbon canohorn (CNH) composites (Zhou et al., 2022). The composite with a CNH mass concentration of 2 wt% (In_2O_3/CNH (2 wt%)) exhibited a high sensor response of 2906 to 2 ppm H_2S at an optimum operating temperature of 70°C. Furthermore, the sensor response of the In_2O_3/CNH (2 wt%) to water vapor with 11%–95% humidity was not over 1.52, indicating that humidity did not significantly affect the sensing performance of the composite to H_2S.

The use of In_2O_3-based nanomaterials as gas sensors has been well established, as discussed in the references above. The development of uniform two-dimensional In_2O_3 nanomaterials may also lead to surprising gas sensing properties due to their large contact surface with air. Additionally, new materials can be explored to establish novel In_2O_3-based composites with heterostructure interfaces, leading to high-performance gas sensors. Careful investigation of the morphology and size effects of the second phase in the composite is essential to screen the best configuration for further improving gas sensing behavior. Machine learning algorithms can be applied to prepare In_2O_3-based gas sensors with excellent selectivity, and assembling several gas sensors in a gas sensor array can build a smart gas sensing system capable of simultaneously detecting several gases under mixed gas atmospheres.

3 Gas sensing mechanism of In_2O_3 nanostructures

Understanding the gas sensing mechanism is crucial for the development of high-performance gas sensors based on In_2O_3. In general, the sensing performance of metal oxide-based sensors is attributed to the redox reaction between the adsorbed oxygen species (O_2^-, O^- and O^{2-}) and the target gas molecules (Wang et al., 2018; Yang et al., 2018; Yang et al., 2019; Wang et al., 2020). For example, flower-like In_2O_3 nanostructure have been shown to exhibit a promising sensor response of 3.1 towards 0.5 ppm isoprene at 190°C (Han et al., 2020). In this case, oxygen gas is adsorbed on the active site, forming the adsorbed oxygen molecule in air (Eq. 1). Electrons are then transferred from the conductive bands of the

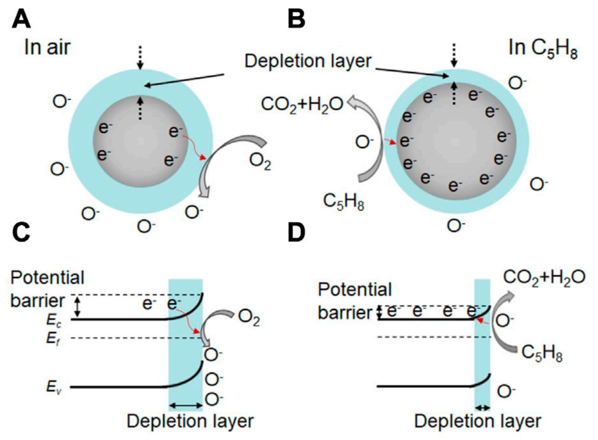

FIGURE 2
(A, B) Schematic diagram of the isoprene sensing mechanism of In_2O_3 nanostructure at 190°C, and the corresponding bending of band structures at the surface region of In_2O_3 nanosturcture **(C, D)**.

flower-like In_2O_3 nanostructure to the adsorbed oxygen molecule, forming adsorbed oxygen species (Eqs. 2–4; Figure 2A). This leads to a bend in the band structure and the formation of a thick space-charge depletion layer at the surface region of the In_2O_3 nanostructure (Figure 2C). Moreover, a high potential barrier is created between the contact flower-like In_2O_3 nanostructure, resulting in a high resistance in air.

$$O_2\ (gas) \rightarrow O_2\ (ads) \tag{1}$$

$$O_2\ (ads) + e^- \rightarrow O_2^-\ (ads)\ (T < 100℃) \tag{2}$$

$$O_2^-\ (ads) + e^- \rightarrow 2O^-\ (ads)\ (100℃ < T < 300℃) \tag{3}$$

$$O^-\ (ads) + e^- \rightarrow O^{2-}\ (ads)\ (T > 300℃) \tag{4}$$

$$C_5H_8\ (gas) \rightarrow C_5H_8\ (ads) \tag{5}$$

$$C_5H_8\ (ads) + 14O^-\ (ads) = 4H_2O + 5CO_2 + 14e^- \tag{6}$$

When the target gas of isoprene is introduced into the testing chamber, the pre-adsorbed oxygen species react with the isoprene molecules (Eqs. 5, 6; Figure 2B), releasing trapped electrons back to the In_2O_3 nanostructure. As a result, the thickness of the space-charge depletion layer decreases (Figure 2D), and the potential barrier is also reduced between the contact flower-like In_2O_3 nanostructure. This process leads to an effective reduction in the resistance of the sensor and a high sensor response to isoprene Similar theories apply to other In_2O_3-based sensors, including Ce-doped In_2O_3 microspheres, CeO_2-loaded In_2O_3 hollow spheres, mesoporous In_2O_3, or Co-doped In_2O_3 nanorods, which exhibit a promising sensing performance to glycol, H_2, ethanol, or HCHO, respectively (Hu et al., 2018b; Liu et al., 2018; Wang et al., 2018; Cheng et al., 2021).

The high specific surface areas of the In_2O_3 nanomaterials have been found to be beneficial in improving the adsorption of gas molecules (Han et al., 2018; Tao et al., 2019; Cao et al., 2020). This increased surface area allows for more gas molecules to access the surface of In_2O_3 nanomaterials, promoting the redox reaction between the adsorbed oxygen species and the target gas molecules. Additionally, the formation of a heterojunction between the main phase of In_2O_3 and the introduced second phase in the composite can promote the transfer of electrons and holes across their surfaces, leading to the bending of their energy bands and the building of a high potential barrier (Du et al., 2015; Ou et al., 2022). Modulating the height of this potential barrier can dramatically change the resistance of the composite, leading to improved sensing performance (Feng et al., 2015). Overall, these two factors are commonly responsible for the high sensing performance of In_2O_3-based composites.

4 Conclusion

In this review, we provide a brief overview of current research on gas sensors based on In_2O_3 nanostructures. Our analysis shows that uniform In_2O_3 nanostructures with high specific surface areas generally exhibit superior gas sensing performance due to enhanced gas molecule adsorption and diffusion. Furthermore, the gas sensing properties of In_2O_3-based materials can be effectively enhanced by creating composites. Adding noble metals is a viable strategy for improving the interaction between gas molecules and In_2O_3, and metal oxides or Mxenes are widely used to further improve the gas sensing properties of In_2O_3 nanostructures. The superior gas sensing performance of composites is primarily attributed to the high specific surface area and the formation of heterojunctions. Therefore, In_2O_3-based materials have immense potential for developing gas sensors with exceptional sensing capabilities.

Author contributions

All authors listed have made a substantial, direct and intellectual contribution to the work, and approved it for publication.

Funding

This work was financially supported by the National Natural Science Foundation of China (Grant Nos. 51802109, 51972102, 52072115, and U21A20500) and the Department of Science and Technology of Hubei Province (Grant No. 2022CFB525).

Conflict of interest

The authors declare that the research was conducted in the absence of any commercial or financial relationships that could be construed as a potential conflict of interest.

Publisher's note

References

Al Shboul, A. M., and Izquierdo, R. (2021). Printed chemiresistive In2O3 nanoparticle-based sensors with ppb detection of H2S gas for food packaging. *ACS Appl. Nano Mater.* 4, 9508–9517. doi:10.1021/acsanm.1c01970

Bai, J., Kong, Y., Liu, Z., Yang, H., Li, M., Xu, D., et al. (2022). Ag modified Tb-doped double-phase In2O3 for ultrasensitive hydrogen gas sensor. *Appl. Surf. Sci.* 583, 152521. doi:10.1016/j.apsusc.2022.152521

Cao, J., Zhang, N., Wang, S., Chen, C., and Zhang, H. (2020). Researching the crystal phase effect on gas sensing performance in In2O3 nanofibers. *Sensors Actuators B Chem.* 305, 127475. doi:10.1016/j.snb.2019.127475

Cheng, P., Wang, Y., Wang, C., Ma, J., Xu, L., Lv, C., et al. (2021). Investigation of doping effects of different noble metals for ethanol gas sensors based on mesoporous In2O3. *Nanotechnology* 32, 305503. doi:10.1088/1361-6528/abf453

Chi, X., Liu, C., Liu, L., Li, S., Li, H., Zhang, X., et al. (2014). Enhanced formaldehyde-sensing properties of mixed Fe2O3–In2O3 nanotubes. *Mat. Sci. Semicon Proc.* 18, 160–164. doi:10.1016/j.mssp.2013.11.016

Cordero, J. M., Borge, R., and Narros, A. (2018). Using statistical methods to carry out in field calibrations of low cost air quality sensors. *Sensors Actuators B Chem.* 267, 245–254. doi:10.1016/j.snb.2018.04.021

Du, H., Wang, J., Sun, Y., Yao, P., Li, X., and Yu, N. (2015). Investigation of gas sensing properties of SnO2/In2O3 composite hetero-nanofibers treated by oxygen plasma. *Sensors Actuators B Chem.* 206, 753–763. doi:10.1016/j.snb.2014.09.010

Feng, C., Li, X., Ma, J., Sun, Y., Wang, C., Sun, P., et al. (2015). Facile synthesis and gas sensing properties of In2O3–WO3 heterojunction nanofibers. *Sensors Actuators B Chem.* 209, 622–629. doi:10.1016/j.snb.2014.12.019

Ge, C., Jin, C., Wang, M., Bai, L., Hussain, S., Qiao, G., et al. (2022). Template-derived net-like SnO2 nanoarrays for robust H2S sensing with broad-range linear response. *Sensors Actuators B Chem.* 366, 131991. doi:10.1016/j.snb.2022.131991

Ge, L., Mu, X., Tian, G., Huang, Q., Ahmed, J., and Hu, Z. (2019). Current applications of gas sensor based on 2-D nanomaterial: A mini review. *Front. Chem.* 7, 839. doi:10.3389/fchem.2019.00839

Han, B., Wang, J., Yang, W., Chen, X., Wang, H., Chen, J., et al. (2020). Hydrothermal synthesis of flower-like In2O3 as a chemiresistive isoprene sensor for breath analysis. *Sensors Actuators B Chem.* 309, 127788. doi:10.1016/j.snb.2020.127788

Han, D., Li, X., Zhang, F., Gu, F., and Wang, Z. (2021). Ultrahigh sensitivity and surface mechanism of gas sensing process in composite material of combining In2O3 with metal-organic frameworks derived Co3O4. *Sensors Actuators B Chem.* 340, 129990. doi:10.1016/j.snb.2021.129990

Han, D., Song, P., Zhang, S., Zhang, H., Xu, Q., and Wang, Q. (2015). Enhanced methanol gas-sensing performance of Ce-doped In2O3 porous nanospheres prepared by hydrothermal method. *Sensors Actuators B Chem.* 216, 488–496. doi:10.1016/j.snb.2015.04.083

Han, D., Zhai, L., Gu, F., and Wang, Z. (2018). Highly sensitive NO2 gas sensor of ppb-level detection based on In2O3 nanobricks at low temperature. *Sensors Actuators B Chem.* 262, 655–663. doi:10.1016/j.snb.2018.02.052

Hu, J., Sun, Y., Xue, Y., Zhang, M., Li, P., Lian, K., et al. (2018). Highly sensitive and ultra-fast gas sensor based on CeO2-loaded In2O3 hollow spheres for ppb-level hydrogen detection. *Sensors Actuators B Chem.* 257, 124–135. doi:10.1016/j.snb.2017.10.139

Hu, X., Zhu, Z., Chen, C., Wen, T., Zhao, X., and Xie, L. (2017). Highly sensitive H2S gas sensors based on Pd-doped CuO nanoflowers with low operating temperature. *Sensors Actuators B Chem.* 253, 809–817. doi:10.1016/j.snb.2017.06.183

Hu, X., Zhu, Z., Li, Z., Xie, L., Wu, Y., and Zheng, L. (2018). Heterostructure of CuO microspheres modified with CuFe2O4 nanoparticles for highly sensitive H2S gas sensor. *Sensors Actuators B Chem.* 264, 139–149. doi:10.1016/j.snb.2018.02.110

Kumar, V., Majhi, S. M., Kim, K. H., Kim, H. W., and Kwon, E. E. (2021). Advances in In2O3-based materials for the development of hydrogen sulfide sensors. *Chem. Eng. J.* 404, 126472. doi:10.1016/j.cej.2020.126472

Li, Z., Liu, X., Zhou, M., Zhang, S., Cao, S., Lei, G., et al. (2021). Plasma-induced oxygen vacancies enabled ultrathin ZnO films for highly sensitive detection of triethylamine. *J. Hazard Mater* 415, 125757. doi:10.1016/j.jhazmat.2021.125757

Liang, X., Kim, T. H., Yoon, J. W., Kwak, C. H., and Lee, J. H. (2015). Ultrasensitive and ultraselective detection of H2S using electrospun CuO-loaded In2O3 nanofiber sensors assisted by pulse heating. *Sensors Actuators B Chem.* 209, 934–942. doi:10.1016/j.snb.2014.11.130

Liu, J., Zhang, L., Fan, J., Zhu, B., and Yu, J. (2021). Triethylamine gas sensor based on Pt-functionalized hierarchical ZnO microspheres. *Sensors Actuators B Chem.* 331, 129425. doi:10.1016/j.snb.2020.129425

Liu, M., Sun, R., Sima, Z., Song, P., Ding, Y., and Wang, Q. (2022). Au-decorated In2O3 nanospheres/exfoliated Ti3C2Tx MXene nanosheets for highly sensitive formaldehyde gas sensing at room temperature. *Appl. Surf. Sci.* 605, 154839. doi:10.1016/j.apsusc.2022.154839

Liu, M., Wang, Z., Song, P., Yang, Z., and Wang, Q. (2021). In2O3 nanocubes/Ti3C2Tx MXene composites for enhanced methanol gas sensing properties at room temperature. *Ceram. Int.* 47, 23028–23037. doi:10.1016/j.ceramint.2021.05.016

Liu, X., Jiang, L., Jiang, X., Tian, X., Sun, X., Wang, Y., et al. (2018). Synthesis of Ce-doped In2O3 nanostructure for gas sensor applications. *Appl. Surf. Sci.* 428, 478–484. doi:10.1016/j.apsusc.2017.09.177

Lu, Z., Zhou, Q., Wei, Z., Xu, L., Peng, S., and Zeng, W. (2019). Synthesis of hollow nanofibers and application on detecting SF6 decomposing products. *Front. Mater.* 6, 183. doi:10.3389/fmats.2019.00183

Luo, Y., An, B., Bai, J., Wang, Y., Cheng, X., Wang, Q., et al. (2021). Ultrahigh-response hydrogen sensor based on PdO/NiO co-doped In2O3 nanotubes. *J. Colloid Interf. Sci.* 599, 533–542. doi:10.1016/j.jcis.2021.04.125

Ma, L., Fan, H., Tian, H., Fang, J., and Qian, X. (2016). The n-ZnO/n-In2O3 heterojunction formed by a surface-modification and their potential barrier-control in methanal gas sensing. *Sensors Actuators B Chem.* 222, 508–516. doi:10.1016/j.snb.2015.08.085

Meng, D., Qiao, T., Wang, G., Shen, Y., San, X., Li, R., et al. (2022). Rational design of CuO/In2O3 heterostructures with flower-like structures for low temperature detection of formaldehyde. *J. Alloys Compd.* 896, 162959. doi:10.1016/j.jallcom.2021.162959

Nikolic, M. V., Milovanovic, V., Vasiljevic, Z. Z., and Stamenkovic, Z. (2020). Semiconductor gas sensors: Materials, technology, design, and application. *Sensors* 20, 6694. doi:10.3390/s20226694

Ou, Y., Zhu, G., Liu, P., Jia, Y., Zhu, L., Nie, J., et al. (2022). Anchoring platinum clusters onto oxygen vacancy-modified In2O3 for ultraefficient, low-temperature, highly sensitive, and stable detection of formaldehyde. *ACS sensors* 7, 1201–1212. doi:10.1021/acssensors.2c00334

Park, S. (2017). Acetone gas detection using TiO2 nanoparticles functionalized In2O3 nanowires for diagnosis of diabetes. *J. Alloys Compd.* 696, 655–662. doi:10.1016/j.jallcom.2016.11.298

Park, S., Sun, G. J., Kheel, H., Lee, W. I., Lee, S., Choi, S. B., et al. (2016). Synergistic effects of codecoration of oxide nanoparticles on the gas sensing performance of In2O3 nanorods. *Sensors Actuators B Chem.* 227, 591–599. doi:10.1016/j.snb.2015.12.098

Peng, B., and Huang, X. (2022). Research status of gas sensing performance of Ti3C2Tx-based gas sensors: A mini review. *Front. Chem.* 10, 1037732. doi:10.3389/fchem.2022.1037732

Phanichphant, S. (2014). Semiconductor metal oxides as hydrogen gas sensors. *Procedia Eng.* 87, 795–802. doi:10.1016/j.proeng.2014.11.677

Shen, Z., Zhang, X., Mi, R., Liu, M., Chen, Y., Chen, C., et al. (2018). On the high response towards TEA of gas sensors based on Ag-loaded 3D porous ZnO microspheres. *Sensors Actuators B Chem.* 270, 492–499. doi:10.1016/j.snb.2018.05.034

Shi, S., Zhang, F., Lin, H., Wang, Q., Shi, E., and Qu, F. (2018). Enhanced triethylamine-sensing properties of P-N heterojunction Co3O4/In2O3 hollow microtubes derived from metal–organic frameworks. *Sensors Actuators B Chem.* 262, 739–749. doi:10.1016/j.snb.2018.01.246

Son, D. N., Hung, C. M., Le, D. T. T., Xuan, C. T., Van Duy, N., Dich, N. Q., et al. (2022). A novel design and fabrication of self-heated In2O3 nanowire gas sensor on glass for ethanol detection. *Sensors Actuators A Phys.* 345, 113769. doi:10.1016/j.sna.2022.113769

Srinivasan, P., Ezhilan, M., Kulandaisamy, A. J., Babu, K. J., and Rayappan, J. B. B. (2019). Room temperature chemiresistive gas sensors: Challenges and strategies—a mini review. *J. Mater. Sci. Mater. Electron.* 30, 15825–15847. doi:10.1007/s10854-019-02025-1

Sui, N., Zhang, P., Zhou, T., and Zhang, T. (2021). Selective ppb-level ozone gas sensor based on hierarchical branch-like In2O3 nanostructure. *Sensors Actuators B Chem.* 336, 129612. doi:10.1016/j.snb.2021.129612

Tao, Z., Li, Y., Zhang, B., Sun, G., Xiao, M., Bala, H., et al. (2019). Synthesis of urchin-like In2O3 hollow spheres for selective and quantitative detection of formaldehyde. *Sensors Actuators B Chem.* 298, 126889. doi:10.1016/j.snb.2019.126889

Van Tong, P., Hoang Minh, L., Van Duy, N., and Manh Hung, C. (2021). Porous In2O3 nanorods fabricated by hydrothermal method for an effective CO gas sensor. *Mater Res. Bull.* 137, 111179. doi:10.1016/j.materresbull.2020.111179

Vuong, N. M., Hieu, N. M., Kim, D., Choi, B. I., and Kim, M. (2014). Ni2O3 decoration of In2O3 nanostructures for catalytically enhanced methane sensing. *Appl. Surf. Sci.* 317, 765–770. doi:10.1016/j.apsusc.2014.08.125

Walker, J. M., Akbar, S. A., and Morris, P. A. (2019). Synergistic effects in gas sensing semiconducting oxide nano-heterostructures: A review. *Sensors Actuators B Chem.* 286, 624–640. doi:10.1016/j.snb.2019.01.049

Wang, J., Zhou, Q., Peng, S., Xu, L., and Zeng, W. (2020). Volatile organic compounds gas sensors based on molybdenum oxides: A mini review. *Front. Chem.* 8, 339. doi:10.3389/fchem.2020.00339

Wang, Z., Hou, C., De, Q., Gu, F., and Han, D. (2018). One-step synthesis of Co-doped In2O3 nanorods for high response of formaldehyde sensor at low temperature. *ACS sensors* 3, 468–475. doi:10.1021/acssensors.7b00896

Wetchakun, K., Samerjai, T., Tamaekong, N., Liewhiran, C., Siriwong, C., Kruefu, V., et al. (2011). Semiconducting metal oxides as sensors for environmentally hazardous gases. *Sensors Actuators B Chem.* 160, 580–591. doi:10.1016/j.snb.2011.08.032

Wu, X., Wang, H., Wang, J., Wang, D., Shi, L., Tian, X., et al. (2022). VOCs gas sensor based on MOFs derived porous Au@ Cr2O3-In2O3 nanorods for breath analysis. *Colloids Surfaces A Physicochem. Eng. Aspects* 632, 127752. doi:10.1016/j.colsurfa.2021.127752

Xu, J. M., and Cheng, J. P. (2016). The advances of Co 3 O 4 as gas sensing materials: A review. *J. Alloys Compd.* 686, 753–768. doi:10.1016/j.jallcom.2016.06.086

Yang, S., Song, Z., Gao, N., Hu, Z., Zhou, L., Liu, J., et al. (2019). Near room temperature operable H2S sensors based on In2O3 colloidal quantum dots. *Sensors Actuators B Chem.* 286, 22–31. doi:10.1016/j.snb.2019.01.110

Yang, W., Feng, L., He, S., Liu, L., and Liu, S. (2018). Density gradient strategy for preparation of broken In2O3 microtubes with remarkably selective detection of triethylamine vapor. *ACS Appl. Mater. interfaces* 10, 27131–27140. doi:10.1021/acsami.8b09375

Zhang, D., Cao, Y., Yang, Z., and Wu, J. (2020). Nanoheterostructure construction and DFT study of Ni-doped In2O3 nanocubes/WS2 hexagon nanosheets for formaldehyde sensing at room temperature. *ACS Appl. Mater. interfaces* 12, 11979–11989. doi:10.1021/acsami.9b15200

Zhang, H., Chen, W. G., Li, Y. Q., and Song, Z. H. (2018). Gas sensing performances of ZnO hierarchical structures for detecting dissolved gases in transformer oil: A mini review. *Front. Chem.* 6, 508. doi:10.3389/fchem.2018.00508

Zhang, Z., Zhu, L., Wen, Z., and Ye, Z. (2017). Controllable synthesis of Co3O4 crossed nanosheet arrays toward an acetone gas sensor. *Sensors Actuators B Chem.* 238, 1052–1059. doi:10.1016/j.snb.2016.07.154

Zhao, R., Wei, Q., Ran, Y., Kong, Y., Ma, D., Su, L., et al. (2021). One-dimensional In2O3 nanorods as sensing material for ppb-level n-butanol detection. *Nanotechnology* 32, 375501. doi:10.1088/1361-6528/ac06f6

Zhou, M., Yao, Y., Han, Y., Xie, L., Zhao, X., Barsan, N., et al. (2022). Ultrasensitive gas sensor based on nanocube In2O3-CNH composite at low operating temperature. *Sensors Actuators B Chem.* 354, 131224. doi:10.1016/j.snb.2021.131224